Dynamic Formation of a Hot Field Reversed Configuration with Improved Confinement by Supersonic Merging of Two Colliding High-β Compact Toroids

M. W. Binderbauer,[1] H. Y. Guo,[1] M. Tuszewski,[1] S. Putvinski,[1] L. Sevier,[1] D. Barnes,[1] N. Rostoker,[1] M. G. Anderson,[1] R. Andow,[1] L. Bonelli,[1] F. Brandi,[2] R. Brown,[1] D. Q. Bui,[1] V. Bystritskii,[1] F. Ceccherini,[1,2] R. Clary,[1] A. H. Cheung,[1] K. D. Conroy,[1] B. H. Deng,[1] S. A. Dettrick,[1] J. D. Douglass,[1] P. Feng,[1] L. Galeotti,[1,2] E. Garate,[1] F. Giammanco,[2] F. J. Glass,[1] O. Gornostaeva,[1] H. Gota,[1] D. Gupta,[1] S. Gupta,[1] J. S. Kinley,[1] K. Knapp,[1] S. Korepanov,[1] M. Hollins,[1] I. Isakov,[1] V. A. Jose,[1] X. L. Li,[1] Y. Luo,[1] P. Marsili,[3] R. Mendoza,[1] M. Meekins,[1] Y. Mok,[1] A. Necas,[1] E. Paganini,[1] F. Pegoraro,[2] R. Pousa-Hijos,[1] S. Primavera,[1] E. Ruskov,[1] A. Qerushi,[1] L. Schmitz,[3] J. H. Schroeder,[1] A. Sibley,[1] A. Smirnov,[1] Y. Song,[1] X. Sun,[1] M. C. Thompson,[1] A. D. Van Drie,[1] J. K. Walters,[1] M. D. Wyman,[1] and the TAE Team

[1]*Tri Alpha Energy, Inc., Post Office Box 7010, Rancho Santa Margarita, California 92688, USA*
[2]*Department of Physics, University of Pisa, Largo B. Pontecorvo 3, 56127 Pisa, Italy*
[3]*Department of Physics and Astronomy, UCLA, Los Angeles, California 90095-1547, USA*
(Received 25 January 2010; published 22 July 2010)

A hot stable field-reversed configuration (FRC) has been produced in the C-2 experiment by colliding and merging two high-β plasmoids preformed by the dynamic version of field-reversed θ-pinch technology. The merging process exhibits the highest poloidal flux amplification obtained in a magnetic confinement system (over tenfold increase). Most of the kinetic energy is converted into thermal energy with total temperature ($T_i + T_e$) exceeding 0.5 keV. The final FRC state exhibits a record FRC lifetime with flux confinement approaching classical values. These findings should have significant implications for fusion research and the physics of magnetic reconnection.

DOI: 10.1103/PhysRevLett.105.045003 PACS numbers: 52.55.Lf, 52.35.Py, 52.35.Vd, 52.55.Ez

The field-reversed configuration (FRC) is a compact toroid (CT) with zero or small self-generated toroidal field [1]. Desirable features of such a configuration for a potential fusion reactor are its simple geometry for ease of construction and maintenance, naturally very high average β (ratio of average plasma to average magnetic pressure inside the separatrix) with moderate field confinement coils and a linear unrestricted divertor, in principle greatly facilitating power, particle and reactor ash removal. In addition, it may allow for the use of advanced, aneutronic fuels such as D-He^3 and p-B^{11}.

The FRC has been produced by various techniques such as field-reversed theta pinch (FRTP) [1,2] with or without translation [3–6], coaxial slow source [7], merging spheromaks with opposite helicities [8,9], and rotating magnetic fields [10–14]. The FRC has demonstrated to be extremely robust in translation [4,5,15]. Recently, the θ-pinch CT merging technique [16–18] has been further explored [19], which takes advantage of the unique translatability of CTs. This allows for the clean and quick capture of the translated CTs in a separate chamber suitable for confinement and steady-state sustainment, which offers a key engineering advantage for potential future fusion reactor designs. This approach may also find applications in other fusion concepts, e.g., as a target plasma for magnetized target fusion.

The C-2 experimental system was built to form high temperature FRCs by merging two θ-pinch preformed high-β plasmoids (Fig. 1). The ultimate goal of C-2 is to sustain hot deuterium FRCs by Neutral Beam Injection (NBI) (with optional additional Rotating Magnetic Field current drive and heating). Suitable target plasma conditions have been achieved in C-2 with record diamagnetic lifetimes of up to 2 ms (as compared to θ-pinch formed and translated FRCs), plasma diameter $\sim$1 m, poloidal flux $\varphi_p \sim 15$ mWb, $\langle\beta\rangle = 2\mu_o\langle p\rangle/\langle B\rangle^2 > 7$ (p is plasma pressure, B is the internal magnetic field), electron density $n_e \sim 10^{20}$ m^{-3}, and total temperature $T_t > 0.5$ keV with $T_t = T_i + T_e$, estimated from radial pressure balance. FRCs are very rugged, surviving extremely dynamic formation, translation and merging processes. This long-lived, stable plasma state exhibits the following key properties: (i) strong flux amplification, exceeding 10 times (during the merging process) the poloidal flux associated with the initial translated individual CTs, (ii) good confinement with flux transport rates significantly below previous FRC scaling [2,20] and approaching classical confinement, (iii) strong conversion from kinetic energy into thermal energy, predominantly into the ion channel. This Letter presents these new advances.

A schematic of C-2 is shown in Fig. 1. C-2 consists of a center confinement vessel, two θ-pinches on opposite sides

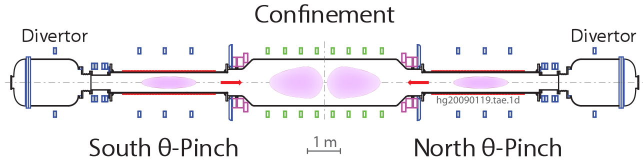

FIG. 1 (color online). Schematic of the C-2 device.

of the confinement chamber, and two divertors at both the north and south ends. The FRCs are produced by colliding and merging two θ-pinch preformed energetic CTs. Figure 2 shows a typical time evolution of the excluded flux radius, $r_{\Delta\phi}$, which approximates the separatrix radius, $r_s \sim r_{\Delta\phi}$, to illustrate the dynamics of the dual CT translation and merging process. The two individual CTs are produced simultaneously and then accelerated out of the respective formation regions at supersonic speeds, $v_Z \sim 250$ km/s, and collide with each other near the midplane at $z = 0$. During the collision the CTs are compressed axially and expand rapidly outwards in the radial direction, followed by axial expansion, before finally settling down into equilibrium. The merging process lasts 10's of μs, i.e., about a few radial Alfvén times (as discussed later). Both radial and axial expansion of the merged FRC are also evidenced by detailed density profile measurements and bolometer-based tomography.

What is remarkable is that the poloidal flux, ϕ_p, increases significantly during the merging process, as illustrated in Fig. 3. The poloidal flux is calculated as $\phi_p = 0.31\pi B_e r_s^3/r_c$, using the Rigid Rotor (RR) assumption, which was found to be consistent with internal probe measurements for translated CTs [5]. Here, B_e is the external magnetic field, r_c is the radius of the metal confinement chamber, which, on the time scale of the experiment, serves as a flux conserver (with an L/R time $\sim$8 ms). As can be seen, the initial individual CTs have relatively small poloidal flux, while the merged FRC exhibits a substantial increase in ϕ_p with a flux amplification factor greater than 10 during the merging process (which occurs at $\sim$30 μs, as highlighted in Fig. 3), significantly larger than in mirror-trapped translated FRCs [5]. The flux amplification factor is the ratio of the poloidal flux of the merged FRC to the average poloidal flux of the two individual translated plasmoids when they first pass (FP) through the midplane, i.e., $2\phi_M/(\phi_N{}^{\rm fp} + \phi_S{}^{\rm fp})$. Note that for spheromak merging, this ratio is found to be unity; i.e., no flux amplification occurs in that case [9]—a key difference between spheromak and FRC merging.

The details of the merging processes are not clear, but it is noteworthy that the final state has very high β; i.e., it is not a Taylor state, which, in principle, is force free and has zero β [21]—a phenomenon observed in astrophysical plasmas and low-β laboratory plasmas [22–25]. The underlying relaxation mechanism in high-β plasmas is, thus, still unclear.

The merged state depends strongly on the translation speed of the initial individual CTs, favoring fast translation, as shown in Fig. 4. C-2 was designed to allow flexible formation schemes, ranging from fully dynamic to static. The most effective way to increase the axial translation speed is by successive energizing of magnetic field coils in the θ-pinch formation sections to rapidly accelerate the CTs out of their respective sources, thus the name dynamic formation. This is in contrast to the static formation scheme, where only the far end formation coils are energized at slightly earlier times to gently push

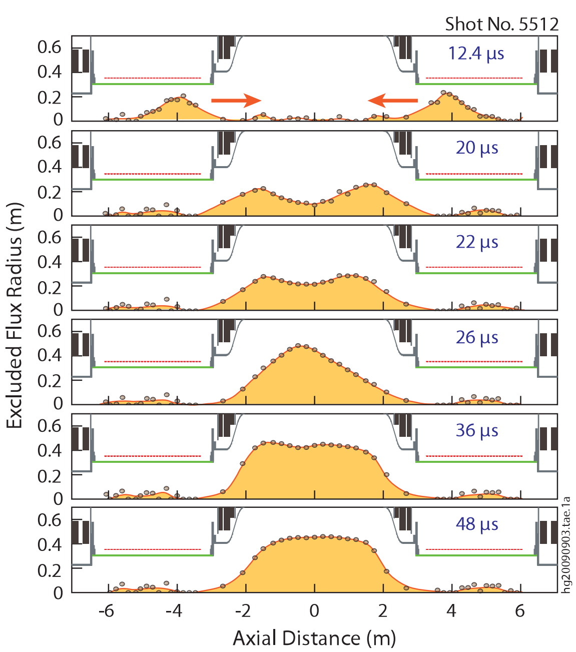

FIG. 2 (color online). Evolution of the excluded flux radius in C-2 obtained from a series of external diamagnetic loops at the two θ-pinch formation sections and magnetic probes embedded inside the central metal confinement chamber. Time is measured from the instant of synchronized field reversal in the θ pinch sources, and distance z is given relative to the center of the confinement chamber.

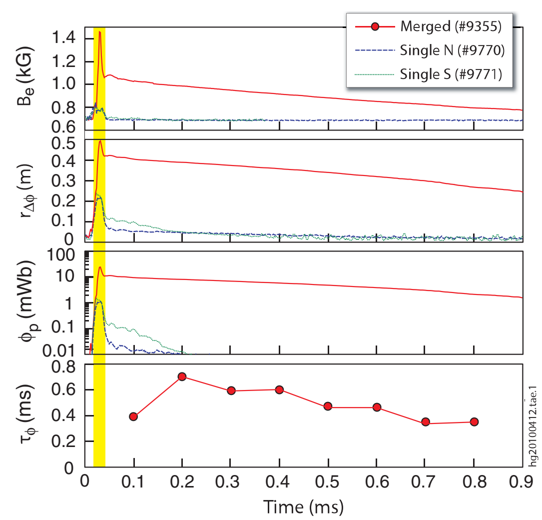

FIG. 3 (color online). Comparison of the initial translated CTs and the resultant merged FRC, showing time traces of the external poloidal field B_e, the excluded flux radius $r_{\Delta\phi}$, and the poloidal flux ϕ_p for individual CTs produced by θ-pinches on the north and south side, respectively, and the result from merging individual CTs formed under identical conditions. Flux decay time, τ_ϕ, for the merged FRC is also shown. Note that the two single CTs were not captured by the end mirrors due to their high translation speeds. Merging occurs around 30 μs, as indicated.

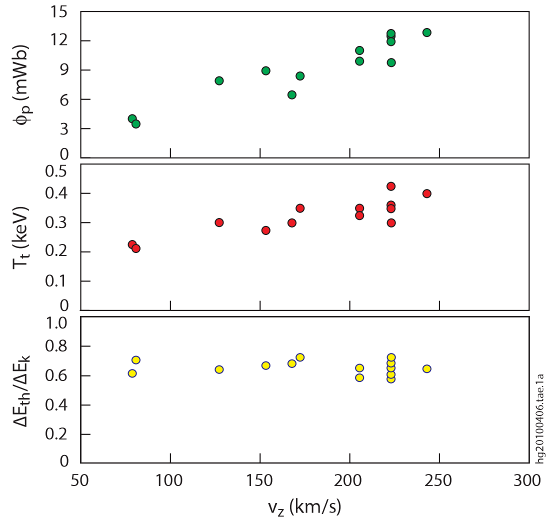

FIG. 4 (color online). Effect of dynamic translation speed. The data are obtained right after merging (~40 μs) of the FRC from a series of reproducible and well-controlled discharges with the same magnetic configurations and gas fuelling rates. The translation speed is varied by energizing the θ-pinch coils at various different times during the initial formation process. Conservation of particle number is assumed.

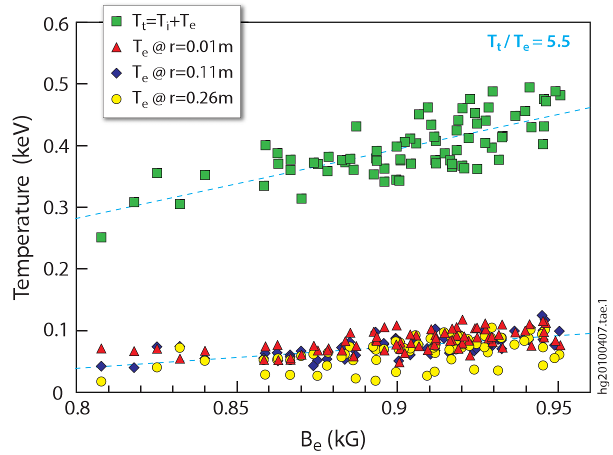

FIG. 5 (color online). T_e determined by Thomson scattering at different radii and T_t derived from the radial pressure balance for typical merged FRC conditions.

the CTs into the confinement chamber. Strong rethermalization occurs during the merging process, converting over 60% of the kinetic energy, $E_k = \frac{1}{2}Nm_i{v_z}^2$ (N is particle number, m_i is ion mass, v_z is axial speed), into plasma thermal energy, $E_{\rm th} = \frac{3}{2}NkT_t$, with the rest going into magnetic energy (manifested by the increase in the poloidal fields). This is also seen in single translated FRCs that are stopped and trapped by end mirrors [3].

As with spheromak merging, strong ion heating also occurs during the FRC merging process. To illustrate this, Fig. 5 shows T_e obtained from multichord Thomson scattering on C-2, along with T_t derived from the radial pressure balance for typical merging FRC conditions. It is found that $T_t \sim 5.5T_e$, consistent with ion temperature measurements derived from Doppler broadening spectroscopy and neutron measurements.

The merged FRC exhibits long lifetimes with a significant improvement in transport properties over the scaling of the conventional θ-pinch formed FRCs [2,20], as discussed later. The dominant global instability seen in the merged FRCs is the $n = 2$ rotational mode, which usually occurs late during the discharge. The $n = 2$ mode is driven by the centrifugal force due to plasma rotation, and is disruptive in θ-pinch formed FRCs, but can be stabilized by applying external static multipole fields [1]. The application of external dc quadrupole fields in C-2 further delays the onset of the $n = 2$ mode, but cannot completely suppress this instability. This is most likely due to the fact that the quadrupole fields become insufficient for stabilization when the plasma radius shrinks.

Figure 6 shows the time evolution of the excluded flux radius, $r_{\Delta\phi}$, the central line-integrated density, $\int n_e d\ell$, and the radial profile contour of the electron density, $n_e(r, t)$, obtained from a multichord HeNe/CO_2 interferometer system located at the midplane, for a merged FRC with the external stabilizing fields being applied. For this particular shot, the onset of the $n = 2$ mode is delayed until ~0.9 ms with the initial stable phase lasting ~500 radial Alfvén times (which is a measure of the MHD time scale for interchange-type modes). The $n = 2$ mode is manifested by the oscillations in the line-integrated density signal, $\int n_e d\ell$, and also seen by tomography as an elliptical distortion of the FRC cross section, rotating in the ion diamagnetic direction with frequencies similar to the ion diamagnetic rotation frequency, i.e., $f_{n=2} \sim \Omega_i^*/2\pi \sim$ 10 kHz for typical FRCs in C-2.

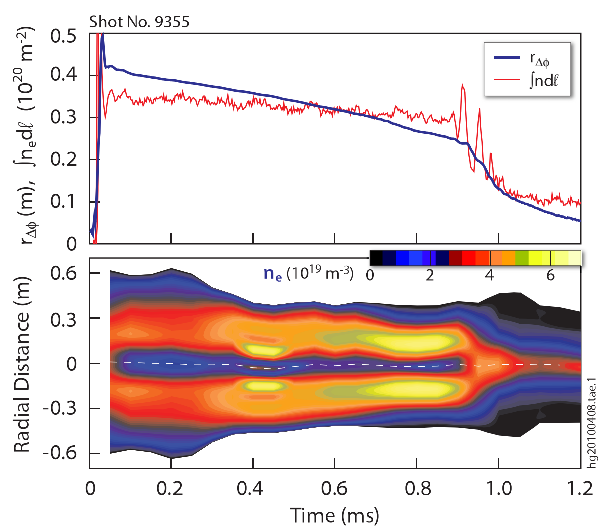

FIG. 6 (color online). Time evolution of the excluded flux radius $r_{\Delta\phi}$ and the line-integrated density $\int n_e d\ell$ at $r =$ 3.3 cm obtained from a six-channel integrated CO_2/HeNe interferometer system (top), and contour of the electron density $n_e(r)$ deduced from the interferometer measurements using the Abel inversion technique (bottom).

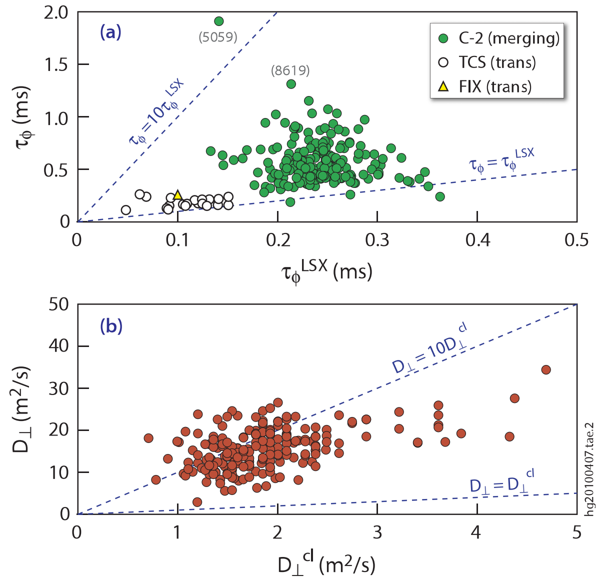

FIG. 7 (color online). (a) Magnetic flux decay time, τ_ϕ, versus the LSX scaling for conventional θ-pinch formed FRCs, τ_ϕ^{LSX}, and results from recent FRC translation experiments, TCS [5] and FIX [3]; (b) diffusivities, $D_\perp$, derived from τ_ϕ, versus classical diffusivities, $D_\perp^{\mathrm{cl}}$, for the well-centered merging FRCs in C-2.

It is noteworthy that during the initial stable phase, the plasma exhibits a hollow density profile with density peaking near the field null ($R = r_s/\sqrt{2}$) as expected from the usual RR profile for an FRC (with the profile parameter $K_{RR} \sim 0.7$). This provides an important verification for the final FRC state resulting from colliding compact toroids, as direct internal probing is not feasible with the hot plasmas in C-2.

The merged FRCs in C-2 also exhibit a remarkable improvement in transport over the conventional θ pinch formed FRC scaling, $\tau_\phi^{\mathrm{LSX}} = 6.52 \times 10^{-5} \rho_L^{-1.07} x_s^{0.5} r_s^{2.14}$ [2], as shown in Fig. 7(a), where ρ_L is the external Larmor radius and $x_s = r_s/r_c$ is the ratio of the separtrix radius to the flux conserver radius. Results from more recent FRC translation experiments are also shown for comparison. The C-2 data are taken during the initial higher confinement phase before the onset of stronger $n = 2$ modes and are limited to well-centered FRCs with horizontal and vertical shifts within 5 cm from the machine's axial centerline. The diffusivity, $D_\perp$, is derived from the flux decay time τ_ϕ as $D_\perp \equiv \eta_\perp/\mu_0 = a^2/\tau_\phi$, as the flux decays on the resistive diffusion time scale. Here $a = r_s - R \approx r_s/4$ is the distance between the field null (R) and the separatrix (r_s) for FRCs. Figure 7(b) compares the transport rates for the merged FRCs with the diffusivities expected from classical transport, i.e., $D_\perp \propto D_\perp^{\mathrm{cl}} = 2D_\parallel^{\mathrm{cl}} \approx 0.45 Z_{\mathrm{eff}} T_t[\mathrm{keV}]^{-3/2}$ [26] for $Z_{\mathrm{eff}} = 1$, and $T_t/T_e = 5.5$ in accordance with the Thomson scattering measurements (Fig. 5). Note that the transport rates may actually be closer to the classical values, if plasma impurities are taken into account.

In summary, high temperature FRCs have been produced in C-2 by supersonic merging of two θ-pinch preformed high-β CTs, achieving record configuration lifetimes with near-classical transport. The formation of a well-confined, high-β plasma state via collisional merging and magnetic reconnection should have significant implications for fusion energy research as well as basic plasma physics.

We thank our shareholders for their support and trust, and the rest of the TAE staff for their dedication, excellent work, and extra efforts. A debt of gratitude is also due to John Slough for his advice during the initial design of C-2.

[1] M. Tuszewski, Nucl. Fusion **28**, 2033 (1988).
[2] A.L. Hoffman and J.T. Slough, Nucl. Fusion **33**, 27 (1993).
[3] H. Himura, S. Okada, S. Sugimoto, and S. Goto, Phys. Plasmas **2**, 191 (1995); M. Inomoto (private communications).
[4] H.Y. Guo, A.L. Hoffman, K.E. Miller, and L.C. Steinhauer, Phys. Rev. Lett. **92**, 245001 (2004).
[5] H.Y. Guo, A.L. Hoffman, L.C. Steinhauer, and K.E. Miller, Phys. Rev. Lett. **95**, 175001 (2005).
[6] D.J. Rej, W.T. Armstrong, and R.E. Chrien *et al.*, Phys. Fluids **29**, 852 (1986).
[7] Z.A. Pietrzyk *et al.*, Nucl. Fusion **27**, 1478 (1987).
[8] Y. Ono, M. Inomoto, Y. Ueda, T. Matsuyama, and T. Okazaki, Nucl. Fusion **39**, 2001 (1999).
[9] C.D. Cothran, A. Falk, A. Fefferman, M. Landreman, and M.R. Brown, Phys. Plasmas **10**, 1748 (2003).
[10] I.R. Jones, Phys. Plasmas **6**, 1950 (1999).
[11] H.Y. Guo, A.L. Hoffman, R.D. Milroy, K.E. Miller, and G.R. Votroubek, Phys. Rev. Lett. **94**, 185001 (2005).
[12] M. Inomoto, K. Kitano, and S. Okada, Phys. Rev. Lett. **99**, 175003 (2007).
[13] S.A. Cohen, B. Berlinger, and C. Brunkhorst *et al.*, Phys. Rev. Lett. **98**, 145002 (2007).
[14] X. Yang, Y. Petrov, and T.S. Huang, Phys. Rev. Lett. **102**, 255004 (2009).
[15] H.Y. Guo, A.L. Hoffman, L.C. Steinhauer, K.E. Miller, and R.D. Milroy, Phys. Rev. Lett. **97**, 235002 (2006).
[16] D.R. Wells, Phys. Fluids **9**, 1010 (1966).
[17] D.R. Wells, J. Davidson, and L.G. Phadke *et al.*, Phys. Rev. Lett. **41**, 166 (1978).
[18] D.R. Wells, P.E. Ziajka, and J.L. Tunstall, Fusion Technol. **9**, 83 (1986).
[19] G. Votroubek, J. Slough, S. Andreason, and C. Pihl, J. Fusion Energy **27**, 123 (2008).
[20] K.F. McKenna, W.T. Armstrong, and R.R. Bartsch *et al.*, Phys. Rev. Lett. **50**, 1787 (1983).
[21] J.B. Taylor, Phys. Rev. Lett. **33**, 1139 (1974).
[22] R.M. Kulsrud, *Plasma Physics for Astrophysics* (Princeton University Press, Princeton and Oxford, 2005).
[23] P.M. Bellan, *Spheromaks* (Imperial College Press, London, 2000).
[24] M. Yamada, J. Geophys. Res. **104**, 14529 (1999).
[25] M.R. Brown, Phys. Plasmas **6**, 1717 (1999).
[26] J. Wesson, *Tokamaks* (Clarendon Press, Oxford, 2004).